

Evaluation of Residual Stress in Stir-squeeze Cast Aluminium – Fly Ash Composites Using X-Ray Diffraction Method

V. Bharathi* and A. R. Anilchandra

B.M.S. College of Engineering, Bengaluru - 560019, Karnataka, India; bharathi.mech@bmsce.ac.in

Abstract

Determination of residual stresses in metals, subjected to secondary processing, is necessary from the point of view of their applications and is widely studied in literature. However, residual stresses induced during service is generally ignored when evaluating the performance of the component. The residual stress in a component could be tensile or compressive in nature and eventually affects its service life under external loading. In this regard, industries demand rapid, efficient, and easier methods of non-destructive testing to identify and control the residual stress in such components. The present work aims at evaluation of residual stress in an LM-25 aluminium alloy/fly Ash Metal Matrix Composites (AMC) after subjecting the specimen to dry sliding wear tests. X-ray diffraction technique was used to measure the residual stress in the “pin” specimen of the pin-on-disc set-up. The residual stress was ~ 24 % higher in the composite compared to the un-reinforced alloy after the wear test while the wear rate, measured in terms of weight loss of the pin, was lower by about 50%, under similar test conditions.

Keywords: AMC, Dry Sliding Wear, Experimental Methods, Residual Stress, Stir-Squeeze Casting, XRD

1.0 Introduction

The quality of the machined specimen, its wear and corrosion resistance is governed by the residual stresses induced during processing. Accurate measurement of residual stress distribution minimizes the cost of manufacturing process. Researchers have proved that compared with unmachined raw components, machined components with compressive residual stress have longer fatigue life. On the other hand, fatigue life of a component is reduced due to tensile residual stresses. Workpiece distortion and dimensional instability are induced in machined components with residual stresses¹. Aluminium Matrix Composites (AMC) are widely used in automobile, industrial and aerospace applications². They are manufactured through different techniques and possess tailored microstructure and mechanical

properties that are best suited for wear applications, such as in brake pads³. Generally Residual Stresses (RS) are induced in a material due to differential cooling; in case of AMCs, the mismatch between the Coefficients of Thermal Expansion (CTE) of the reinforcing phase and matrix phase is the primary reason for residual stress during fabrication of composites⁴. Influence of residual stress on the wear mechanisms and wear rate in AMCs is documented in the literature⁵. A pin-on-disc test set-up is the widely used approach to perform sliding wear studies. Residual Stresses (RS) are the “self-balanced” and “non-homogenous” stresses that are generated and trapped during different manufacturing processes⁶⁻⁹. These stresses remain within a material after the manufacturing stage, when there is neither thermal gradient nor external force¹⁰⁻¹³. However, during sliding contact, the residual stress profiles and its magnitude are altered over the

*Author for correspondence

course of operation, which significantly affects the products' performance: in the pin-on-disc wear study, it is the RS induced due to wear on the life and performance of the 'pin' which is tantamount to 'brake-pad' in automobile applications. It was observed that the forces generated on a fixed boundary condition lead to residual stresses which are totally different from normal stresses¹⁴. Macro residual stresses vary on the scale of individual grain and are caused by crystalline defects. Depending on the nature of the residual stress (tensile or compressive), various analytical and experimental methods are available to determine their magnitude: X-ray diffraction method is exclusively used to measure the residual stresses more accurately¹⁵. Evolution of wear-induced residual stresses in sliding contact has received little attention and is the focus of the present work.

2.0 Materials and Methods

LM – 25 aluminium alloy was reinforced with 7.5 wt. % of fly ash during stir casting followed by squeeze casting to fabricate the AMC using a 20-tonne hydraulic squeeze press as shown in Figure 1.

During the process a pressure was maintained at 50 kg/cm² was maintained for a duration of 15 minutes. Dry sliding wear tests were carried out using pin-on-disc

setup by varying normal load, sliding velocity and sliding distance according to the experiments framed as per L-27 orthogonal array. The amount of wear was recorded in terms of weight loss in kg. The experiments were carried out for base metal and composite and the results were tabulated^{16,17}. The results from L-27 orthogonal array tests are shown in Figure 2 and its validation is shown in Figure 3 respectively. Validation trials were conducted for the intermediate values of the process parameters to assess the precision and accuracy of the regular results shown in Figure 2.

From the Figure 2, it is evident that wear resistance is low for the base metal and increased in the composite. Consistently the composite shows the higher wear resistance under all test conditions. This is because: hardness of the fly ash particles embedded in the soft ductile aluminium matrix contributes for the enhancement of the wear resistance of the composite^{7,8}. It also bears load transferred from the matrix material.

In order to validate the observed trend in Figure 2, certain trials of experiments were intermittently picked and their results of wear resistance is shown in Figure 3. Similar trend was observed for the changed wear test parameters wherein AMC exhibits higher wear resistance compared to unreinforced LM – 25¹⁸

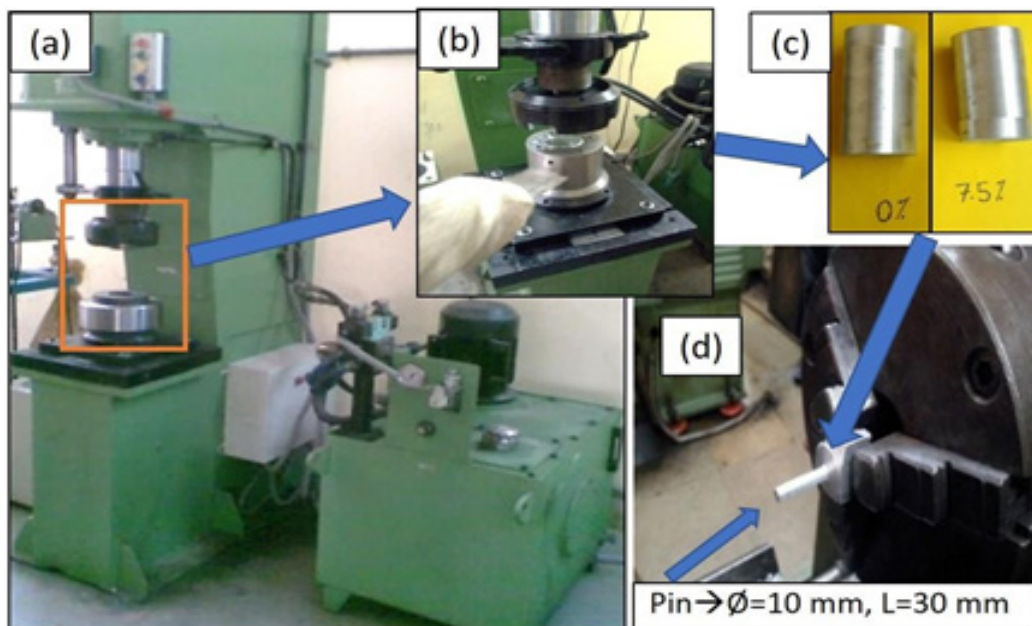


Figure 1. (a) Squeeze Casting setup (b) cast billet inside the set-up (c) finished cast alloy LM25 and composite (d) pin-on-disc specimen preparation and its dimensions.

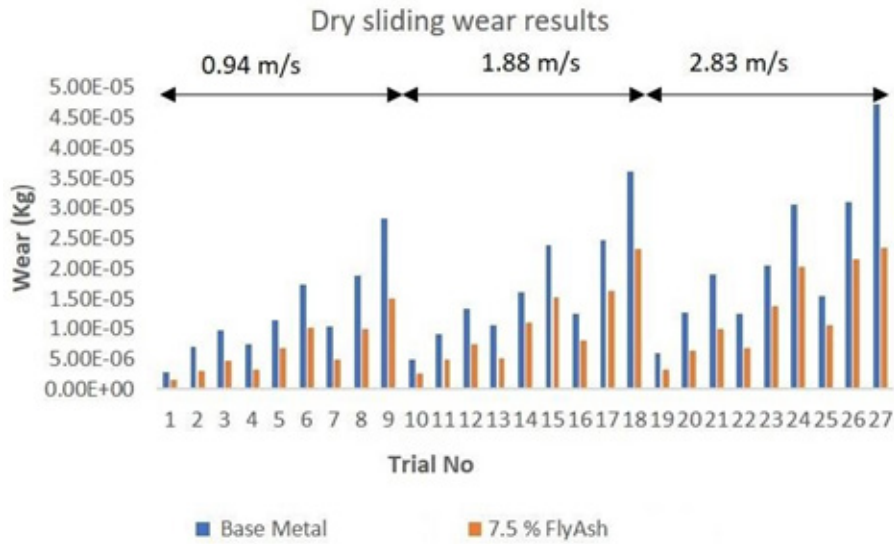


Figure 2. Bar chart for dry sliding wear behaviour of base metal (LM – 25) and 7.5% fly ash reinforced AMC: for three loading conditions (4.5, 9.8, 14.7 N) and three sliding distances (1, 2, 3 km).

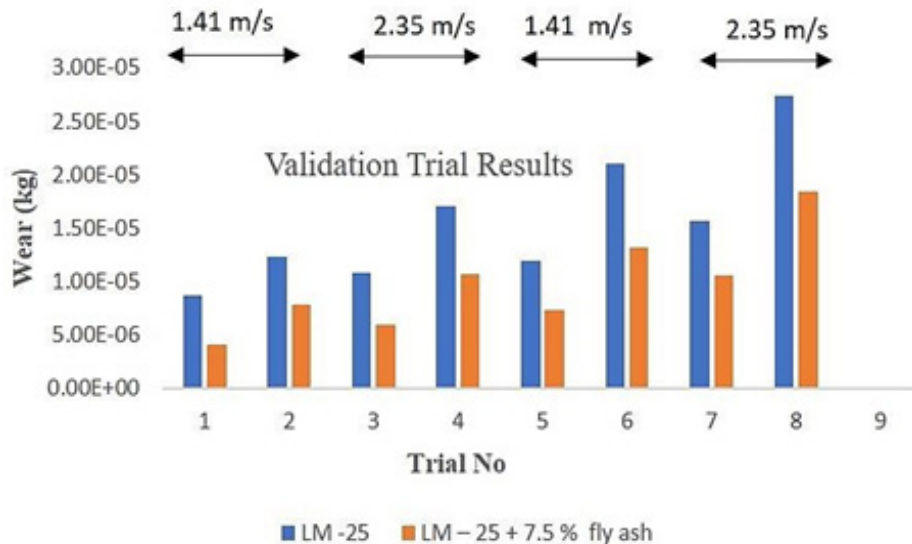


Figure 3. Bar chart for dry sliding wear behaviour of base metal (LM – 25) and 7.5% fly ash reinforced AMC: for two loading conditions (7.15, 12.25 N) and two sliding distances (1.5, 2.5 km).

2.1 SEM and EDS Studies

EDS analysis was carried out to ascertain the chemical compositions of the base metal, fly ash and 7.5% fly ash reinforced AMCs. Before and after the wear test all the constituent elements that were measured using EDS analysis were on par with the matrix and reinforcement

materials used in the investigation. Figure 4, 5 and 6 represent SEM images and EDS analyses of base metal, fly ash particles and 7.5% fly ash reinforced composites respectively. Base metal represents higher peak for aluminium followed by smaller peaks for silicon and magnesium whereas fly ash represents higher peak

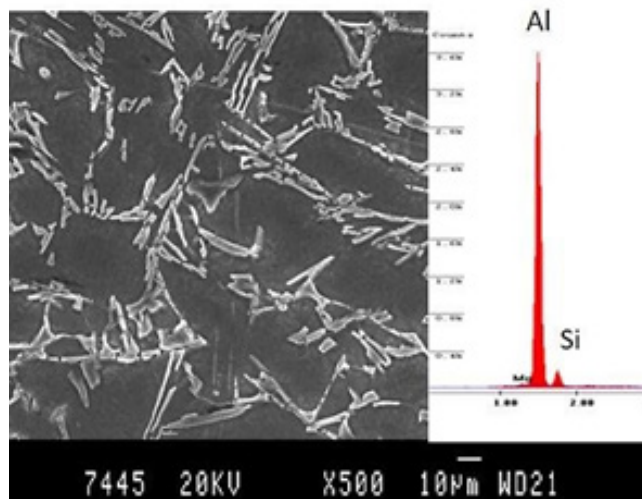


Figure 4. SEM image of base metal LM-25 highlighting the silicon needle structure: The inset image shows EDS analysis.

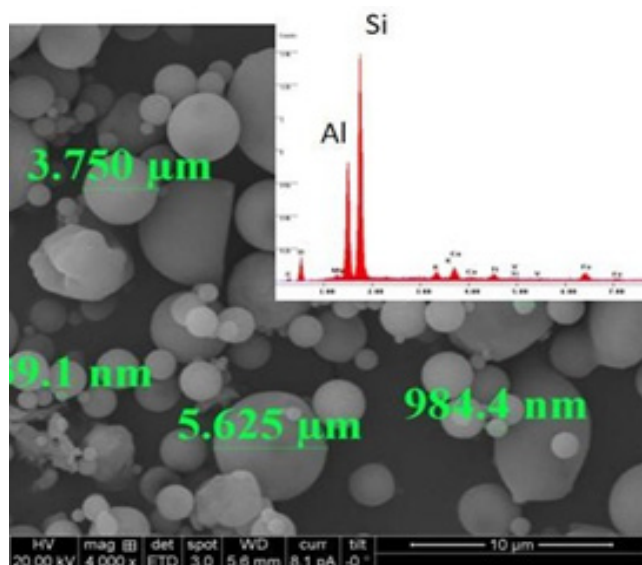


Figure 5. SEM image for fly ash reinforcement particles: Inset image shows the EDS analysis for fly ash particles.

for silicon followed by comparatively smaller peak for aluminium and magnesium content. Presence of silicon content in the matrix as well as reinforcement material symbolizes its contribution for the increased hardness of the composite. EDS analysis of the base metal and the composite clearly indicate the presence of higher aluminium peak, lower silicon peak and lower intensity in magnesium peak. No iron content was recorded in the EDS analyses of base metal and the composite, clearly

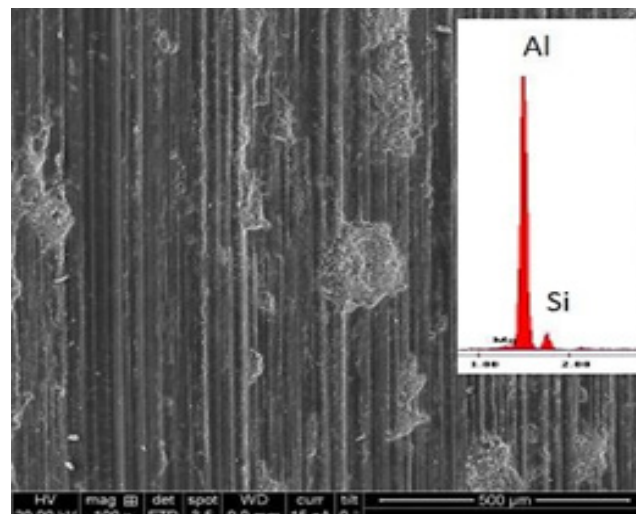


Figure 6. SEM image of wear tested 7.5% fly ash reinforced AMC subjected to dry sliding at 4.5 N, 3000 m and 0.9423 m/s: Inset image shows EDS analysis for 7.5% fly ash reinforced aluminium matrix composite

indicating no transfer of counterpart material onto the pin specimen and is shown in Figure 6.

2.2 Results of XRD Studies

The Figures 7(a) and 7(b) represent XRD results of base metal and 7.5% fly ash reinforced composite respectively. Through XRD results it is revealed that for base metal LM – 25, the highest peaks formed represent Spinel (aluminium magnesium oxide) and Berlinite (aluminium phosphorous oxide) compound formation and is an established procedure. XRD analysis of 7.5% fly ash reinforced AMC shows the dispersion of fly ash in LM – 25 matrix material. With the increasing sliding speed, the rotating disc reacts with atmospheric oxygen to form various oxides along with compounds of aluminium resulting in yielding of Mechanical Mixing Layer

– MML between the composite pin and the disc¹⁹. This enhances the work hardening of the aluminium during the sliding action: formation of various oxides on the surface of the composite pin enhances the wear resistance. The oxide layers formed act like barrier and protect composite from further oxidation. But, the interfacial bonding between the aluminium and fly ash of the composite will be lowered due to thermal softening at higher speed and load conditions. The protective barrier that breaks down during the sliding action results in greater wear loss. This indicates clear transition of wear regime from mild

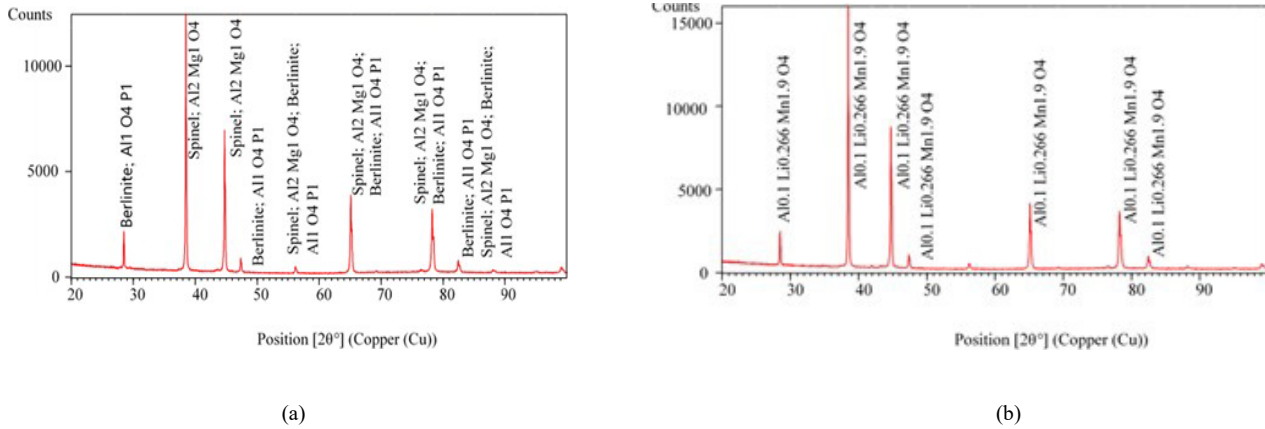


Figure 7. (a). XRD graph for base metal LM-25 at 14.7 N load, 0.9423 m/s sliding velocity and 2000 m of sliding distance. (b). XRD graph for 7.5% fly ash reinforced aluminium matrix composite at 14.7 N load, 0.9423 m/s sliding velocity and 2000 m of sliding distance.

to severe with increased load and sliding distance. Since from EDS analyses there was no record of iron content, formation of iron oxide was also not seen in XRD analyses of both base metal and the composite.

2.3 Residual Stress Measurement

Surface stress analysis using X-ray diffraction technique was carried out at Advanced Machine Tool Testing Facility (AMTTF) CMTI, Bengaluru. X-ray diffraction was used to measure residual stress using the distance between crystallographic planes, i.e., d-spacing. When the material is in tension, the d-spacing increases and, when under compression the d-spacing decreases.

This principle is used to measure the induced stresses. The equipment was initialized for about 15 minutes to warm up the system and the X-ray tube was excited to an appropriate level before starting the measurements. The test piece was placed on a suitable fixture and the area where the stress analysis had to be carried out was focused manually in the equipment. The measurement was carried out by setting the parameters in accordance with details of the test sample. The inputs were supplied as required for the test e.g., time of exposure, Beta and phi angles, no. of averages etc., and the final measurement was carried out. The measurement setup along with the mounted specimen is shown in Figure 8.

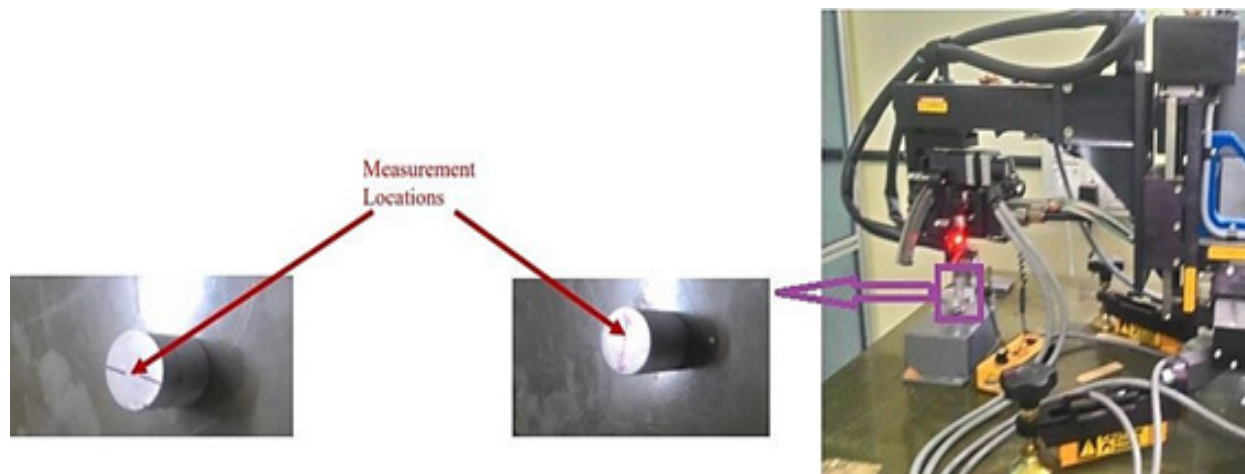


Figure 8. Setup for the measurement of residual stresses highlighting the specimen and Measurement Locations (On the Marked targets).

3.0 Results and Discussion

X-Ray Diffraction to determine the strains and stresses in the specimen is based on Bragg’s law. Two detectors

that are normal to the incident beam record the Debye rings, which are seen as circular intensity rings in the transmitted diffracted beams. The application of stress changes the d-spacing, leading to the distortion of these

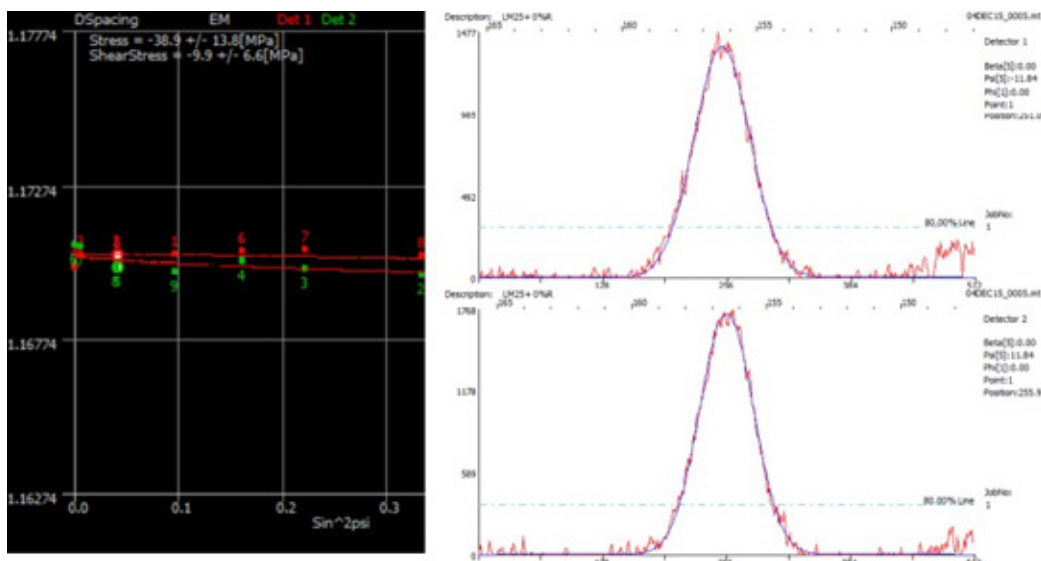


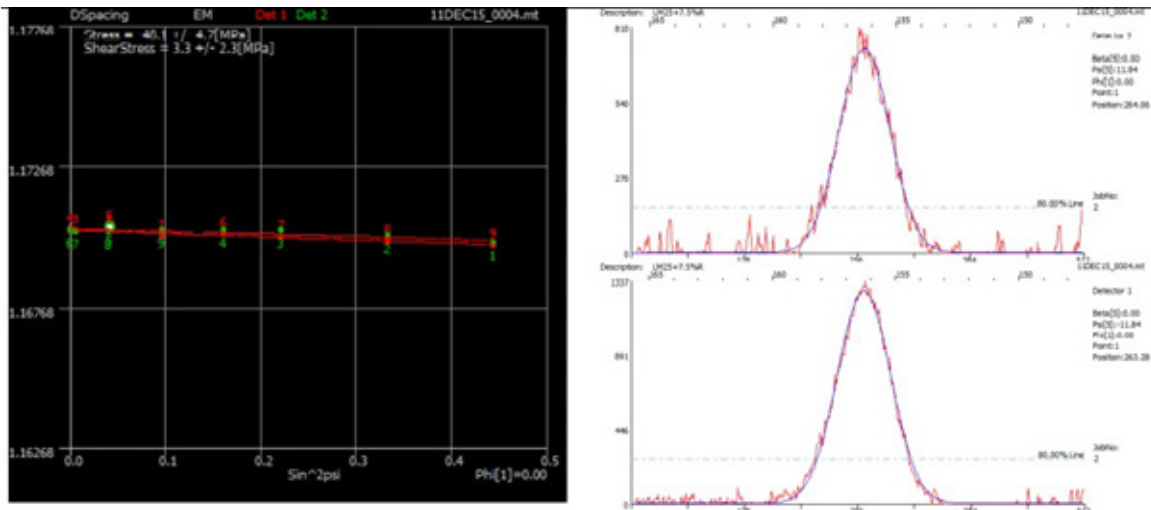
Figure 9. Representation of residual stress in LM – 25 alloy.

Table 1. Residual stress measurement values for LM – 25 alloy

BASE METAL LM – 25			
RSalloy = - 38.9 ± 13.8 MPa			
Shear Stress = 9.9 ± 6.6 MPa			
Intensity Ratio	2.28	2.07	
Average peak breadth	2.54 ± 0.21	2.45 ± 0.21	
Average peak FWHM	2.349 ± 0.25	2.335 ± 0.26	
Detector 1		Detector 2	
d spacing	FWHM	d spacing	FWHM
1.170459	2.769	1.169696	2.067
1.170479	2.639	1.169841	2.145
1.170504	2.551	1.170026	2.093
1.170070	2.298	1.170264	2.108
1.170443	2.304	1.170071	2.323
1.170568	2.226	1.170778	2.473
1.170637	2.198	1.170709	2.523
1.170453	2.039	1.170069	2.466
1.170290	2.113	1.169696	2.416

Table 2. Residual stress measurement values for LM – 25 alloy reinforced with 7.5 wt.% fly ash

LM – 25 + 7.5 % Fly ash reinforced composite			
RS _{AMC} = - 48.1 ± 4.7 MPa			
Shear Stress = 3.3 ± 2.3 MPa			
Intensity Ratio	2.42	2.33	
Average peak breadth	2.54 ± 0.12	2.53 ± 0.22	
Average peak FWHM	2.408 ± 0.16	2.428 ± 0.24	
Detector 1		Detector 2	
d spacing	FWHM	d spacing	FWHM
1.170193	2.622	1.169963	2.224
1.170325	2.587	1.170177	2.240
1.170390	2.553	1.170398	2.206
1.170442	2.414	1.170378	2.305
1.170505	2.453	1.170466	2.274
1.170220	2.379	1.170359	2.462
1.170119	2.239	1.170323	2.552
1.169965	2.257	1.170331	2.675
1.169862	2.168	1.170367	2.914

**Figure 10.** Representation of residual stress in LM – 25 alloy reinforced with 7.5 wt.% fly ash.

Debye rings at the detector. The degree of distortion in the direction of applied stress provides a reasonable estimation of the lattice strain.

Tables 1 and 2 show the residual stress measurement values for LM – 25 alloy and 7.5 wt.% fly ash reinforced composite respectively. All values from both the detectors

were recorded and tabulated. Figures 9 and 10 represent the plot recorded by the two detectors with d- spacing for the alloy and the composite respectively

It was observed that the residual stresses were of compressive in nature where shear stress factor was low in case of composite compared with base metal. This is due to the contribution of the reinforcement particles in bearing the load effectively. Compared to the alloy, the AMC showed higher residual stress after the wear test under similar wear testing conditions. The calculation of percentage increase in the residual stress in AMC is as follows:

$$\% \text{ increase in RS} = [\text{mod}(\text{RS}_{\text{AMC}} - \text{RS}_{\text{Alloy}})] / \text{RS}_{\text{Alloy}}$$

The values of RS_{Alloy} and RS_{AMC} are provided in the Table 1 and 2 respectively.

4.0 Conclusion

The present work highlights the measurement of residual stress in an LM-25 aluminium alloy/7.5% fly Ash Metal Matrix Composites (AMC) fabricated by stir casting followed by squeeze casting. The residual stresses were measured on both the alloy and composite specimen after the pin-in-disc dry sliding wear test. X-ray diffraction technique was used to measure the residual stress in the “pin” specimen of the pin-on-disc set-up.

The wear rate, measured in terms of weight loss of the pin, was lower by about 50%, under similar test conditions in the composite compared to the unreinforced alloy.

- The residual stress was about 24% higher in the composite compared to the un-reinforced alloy after the wear test.
- The effect of wear induced residual stress on the subsequent wear behaviour is yet to be ascertained and is under consideration for future work.

5.0 References

1. Carpenter HW, Paskaramoorthy R, Reid RG. The effect of residual stresses and wind configuration on the allowable pressure of thick-walled GFRP pipes with closed ends. *Int J Mech Mater Des.* 2015; 11:455-462 <https://doi.org/10.1007/s10999-014-9280-z>
2. Sharma A, Kar A, Kumar S. A critical review on recent advancements in aluminium-based metal matrix composites. *Crystals -Material Science Engineering.* 2024; 14:1-42. <https://doi.org/10.3390/cryst14050412>
3. Akanksh VN, Hegde P, Manjunath AB, Nagaral M, Siddharth S, Siddaraju C. Microstructural characterization, mechanical and wear behaviour of Al2024-B4C composites for aerospace applications. *J Mines Met Fuels.* 2022; 70(3A):138-142. <https://doi.org/10.18311/jmmf/2022/30683>
4. Bruno G, Fernández R, González-Doncel G. Correlation between residual stresses and the strength differential effect in PM 6061Al-15 vol% SiCw composites: Experiments, models and predictions. *Acta Materialia.* 2004; 52(19):5471-5483. <https://doi.org/10.1016/j.actamat.2004.08.005>
5. Chuard M, Mairey D, Mignot J, Sprauel JM, Tribol J. Study of residual stresses induced by sliding wear. *J Tribol.* 1985; 107(2):195-199. <https://doi.org/10.1115/1.3261019>
6. Outeiro JC. 11 - residual stresses in machining, mechanics of materials in modern manufacturing methods and processing techniques. Amsterdam: Elsevier; 2020. p. 297-360. <https://doi.org/10.1016/B978-0-12-818232-1.00011-4>
7. Liu ZQ, Pan YZ, Tang ZT et al. The influence of tool flank wear on residual stresses induced by milling aluminum alloy. *J Mater Process Technol.* 2009; 209(9):4502-4508. <https://doi.org/10.1016/j.jmatprotec.2008.10.034>
8. Bharathi V, Ramachandra M, Srinivas S. Influence of fly ash content in aluminium matrix composite produced by stir-squeeze casting on the scratching abrasion resistance, hardness and density levels. *Mater Today Proc.* 2017; 4(8):7397-7405. <https://doi.org/10.1016/j.matpr.2017.07.070>
9. Khodake PM, Mankar DS. Residual stress produced after machining in mechanical components and its effects on fatigue life: A state of art. *Int J Mech Prod Eng Res Dev.* 2015; 5(1):1-10.
10. Akbari S, Shokrieh MM, Taheri-Behrooz F. Characterization of residual stresses in a thin-walled filament wound carbon/epoxy ring using incremental hole drilling method. *Compos Technol.* 2014; 94:8-15. <https://doi.org/10.1016/j.compscitech.2014.01.008>
11. Apel D, Bruno G, Evans A, Fritsch T, Hesse R, Kromm A, Mishurova T, Serrano-Munoz I, Trofimov A, Ulbricht A. On the interplay of microstructure and residual stress in LPBF IN718. *J Mater Sci.* 2021; 56:5845-5867. <https://doi.org/10.1007/s10853-020-05553-y>
12. Batish A, Kumar S, Sidhu S. Analysis of residual stresses in particulate reinforced aluminium matrix composite

- after EDM. *Mater Sci Technol.* 2015; 31(15):1850-1859. <https://doi.org/10.1179/1743284715Y.0000000033>
13. Evsevlev S, Mishurova T, Sevostianov I, *et al.*, Explaining deviatoric residual stresses in aluminum matrix composites with complex microstructure. *Metall Mater Trans A.* 2020; 51: 3104-3113. <https://doi.org/10.1007/s11661-020-05697-1>
 14. Carpenter HW, Paskaramoorthy R, Reid RG. The effect of Residual stresses and wind configuration on the allowable pressure of thick walled GFRP pipes with closed ends. *Int J Mech Mater Des.* 2015; 11:455-462. <https://doi.org/10.1007/s10999-014-9280-z>
 15. Tabatabaeian A *et al.* Residual stress in engineering materials: A Review. *Adv Eng Mater.* 2021; 24(3):1-65. <https://doi.org/10.1002/adem.202100786>
 16. Bharathi V, Ramachandra M, Srinivas S. Mathematical modeling of dry sliding wear behaviour of stir - squeeze cast aluminium matrix composite. *IOP Conf Series: Materials Science and Engineering.* 2018; 455:1-12. <https://doi.org/10.1088/1757-899X/455/1/012008>
 17. Ramachandra M, Radhakrishna K. Effect of reinforcement of fly ash on sliding wear, slurry erosive wear and corrosive behaviour of aluminium matrix composite. *Wear.* 2007; 1450-1462. <https://doi.org/10.1016/j.wear.2007.01.026>
 18. Meher A, Mahapatra MM, Samal P, Vundavilli PR. Recent progress in aluminum metal matrix composites: A review on processing, mechanical and wear properties. *J Manuf Process.* 2020; 59:131-152. <https://doi.org/10.1016/j.jmapro.2020.09.010>
 19. Sundararajan G, Venkataraman B. Correlation between the characteristics of the mechanically mixed layer and wear behaviour of aluminium. Al-7075 alloy and Al-MMCs, *Wear.* 2000; 245(1-2):22-38. [https://doi.org/10.1016/S0043-1648\(00\)00463-4](https://doi.org/10.1016/S0043-1648(00)00463-4)